DOI: 10.1002/ejic.200800299

Bis(cycloheptatrienyl) Derivatives of the First-Row Transition Metals: Variable Hapticity of the Cycloheptatrienyl Ring

Hongyan Wang,*[a,b] Yaoming Xie,[b] R. Bruce King,*[b] and Henry F. Schaefer III[b]

Keywords: Cycloheptatrienyl derivatives / Sandwich compounds / Density functional theory

Extrapolation from ferrocene and dibenzenechromium suggests the currently unknown 18-electron sandwich compound $(\eta^7\text{-}C_7H_7)_2Ti$ as a possible stable molecule. However, density functional theory (DFT) methods using the B3LYP and BP86 functionals predict $(\eta^7\text{-}C_7H_7)_2Ti$ to distort by ring slippage to give a singlet 16-electron complex $(\eta^7\text{-}C_7H_7)\text{-}Ti(\eta^5\text{-}C_7H_7)$ having an uncomplexed C=C double bond in one of the C_7H_7 rings but otherwise closely related to the known $(\eta^7\text{-}C_7H_7)Ti(\eta^5\text{-}C_5H_5)$. The situation is similar with $(C_7H_7)_2V$ except that the corresponding structures have doublet spin multiplicity. However, an analogous $(\eta^7\text{-}C_7H_7)\text{-}Cr(\eta^5\text{-}C_7H_7)$ structure is not found for chromium. Instead the most stable $(C_7H_7)_2Cr$ structure is a singlet d^0 six-coordinate formally Cr^{VI} complex with two tridentate cyclopropyldivinyl C_7H_7 ligands. The latter rearrangement of the C_7H_7 rings bonded to chromium can involve initially a $(\eta^6\text{-}C_7H_7)_2Cr$ diradical sandwich compound followed by a bis(η^5-norcaradienyl)Cr intermediate. For the later first-row transition metals the lowest energy $(C_7H_7)_2M$ structures are predicted to be doublet $(\eta^7\text{-}C_7H_7)Mn(\eta^3\text{-}C_7H_7)$ rather than $(\eta^5\text{-}C_7H_7)_2Mn$ for manganese, singlet *cis* and *trans* structures $(\eta^5\text{-}C_7H_7)_2Fe$ for iron, doublet $(\eta^3\text{-}C_7H_7)_2Co$ for cobalt, and two singlet $(\eta^3\text{-}C_7H_7)_2Ni$ stereoisomers for nickel.

1. Introduction

The landmark discovery of the sandwich compound ferrocene,[1,2] $(\eta^5\text{-}C_5H_5)_2Fe$ (Figure 1) in 1951 stimulated the rapid subsequent development of transition metal organometallic chemistry. A subsequent milestone was the discovery of the related sandwich compound dibenzenechromium,[3] $(\eta^6\text{-}C_6H_6)_2Cr$ in 1955 (Figure 1). At that time the idea of sandwiching a chromium atom between two stable benzene molecules to give a thermally stable sandwich compound was truly revolutionary.

The stabilities of ferrocene and dibenzenechromium relate at least partially to the favorable 18-electron configuration of the central metal atom. Extrapolation to sandwich compounds with larger carbocyclic ring sizes and the favorable 18-electron configuration suggests bis(cycloheptatrienyl)titanium, $(\eta^7\text{-}C_7H_7)_2Ti$ (Figure 1) as a stable molecule. However, during the more than half century since the discovery of ferrocene this sandwich compound has never been prepared even though the sandwich compound dibenzenetitanium, $(\eta^6\text{-}C_6H_6)_2Ti$, with a normally less favorable 16-electron configuration, is known.[4,5] This suggests an inherent instability of $(\eta^7\text{-}C_7H_7)_2Ti$.

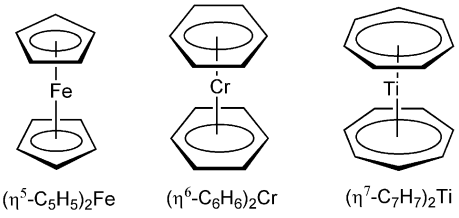

Figure 1. Some sandwich compounds with 18-electron metal configurations.

This apparent instability of $(\eta^7\text{-}C_7H_7)_2Ti$ cannot arise from any inherent problems with the $\eta^7\text{-}C_7H_7M$ bond because numerous derivatives of this type are known.[6] The first such $\eta^7\text{-}C_7H_7M$ complex was the cation $(\eta^7\text{-}C_7H_7)\text{-}Mo(CO)_3^+$ (Figure 2), prepared in 1958[7,8] by the hydride abstraction from the triene complex $(\eta^6\text{-}C_7H_8)Mo(CO)_3$. Shortly thereafter, the neutral sandwich compound[9,10] $(\eta^5\text{-}C_5H_5)V(\eta^7\text{-}C_7H_7)$ was obtained from the thermal reaction of cycloheptatriene with $(\eta^5\text{-}C_5H_5)V(CO)_4$.

Another feature of the cycloheptatrienyl ligand is its ability to form metal complexes involving only partial bonding of the seven-membered ring to the metal atom. Early examples of such complexes are the trihapto derivatives[11–13] $(\eta^5\text{-}C_5H_5)Mo(CO)_2(\eta^3\text{-}C_7H_7)$ and $(\eta^3\text{-}C_7H_7)Co(CO)_3$ (Figure 3), in which the four carbon atoms of the C_7H_7 ring not bonded to the metal atom can be regarded as a 1,3-diene

[a] College of Sciences, Southwest Jiaotong University, Chengdu 610031, P. R. China
[b] Department of Chemistry and Center for Computational Chemistry, University of Georgia, Athens, Georgia 30602, USA
E-mail: wanghyxx@yahoo.com
rbking@chem.uga.edu

Supporting information for this article is available on the WWW under http://www.eurjic.org or from the author.

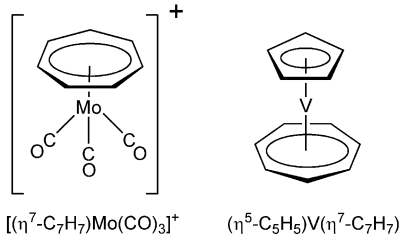

$[(\eta^7\text{-}C_7H_7)Mo(CO)_3]^+$ $(\eta^5\text{-}C_5H_5)V(\eta^7\text{-}C_7H_7)$

Figure 2. Some early η^7-C_7H_7M derivatives.

unit with corresponding carbon–carbon distances reflecting alternating single and double bonds. More recently pentahapto cycloheptatrienyl derivatives[14] such as η^5-$C_7H_7Mn(CO)_3$ (Figure 4, a) and monohapto cycloheptatrienyl derivatives[15,16] such as η^1-$C_7H_7Re(CO)_5$ (Figure 4, b) have also been prepared.

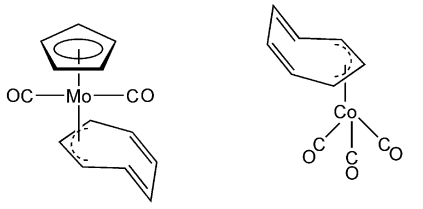

$(\eta^5\text{-}C_5H_5)Mo(CO)_2(\eta^3\text{-}C_7H_7)$ $(\eta^3\text{-}C_7H_7)Co(CO)_3$

Figure 3. Some early η^3-C_7H_7M derivatives: (a) $(\eta^5\text{-}C_5H_5)Mo(CO)_2(\eta^3\text{-}C_7H_7)$; (b) $(\eta^3\text{-}C_7H_7)Co(CO)_3$.

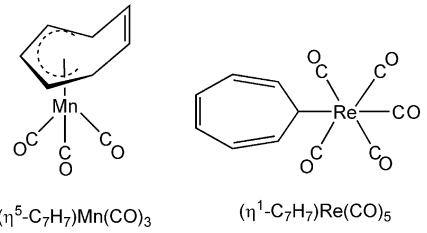

$(\eta^5\text{-}C_7H_7)Mn(CO)_3$ $(\eta^1\text{-}C_7H_7)Re(CO)_5$

Figure 4. Examples of η^5-C_7H_7 and η^1-C_7H_7 derivatives.

An interesting question is the nature of the η^7-C_7H_7–metal bond. Originally such compounds were assumed to be metal complexes of the tropylium ion, $C_7H_7^+$, a planar aromatic species with 6 π electrons isoelectronic with benzene. However, early work by Wilkinson and co-workers[17] suggested that reactions of tropylium salts with transition-metal derivatives were rarely suitable for the preparation of η^7-C_7H_7 metal complexes. More recent studies on η^7-C_7H_7–metal complexes suggest preferred formulations of such complexes as derivatives of the 10 π-electron trianion[18–21] $C_7H_7^{3-}$, which has been generated in a metal-free form by the treatment of 1,4-cycloheptadiene with *n*BuLi.[22,23] Thus the metal formal oxidation states in the known mixed sandwich complexes $(\eta^5\text{-}C_5H_5)M(\eta^7\text{-}C_7H_7)$ (M = Ti, V, Cr) may be considered to be +4 in contrast to the formal zero metal oxidation states in the isoelectronic and isomeric dibenzene-metal complexes $(\eta^6\text{-}C_6H_6)_2M$ (M = Ti, V, Cr). This may account for the experimentally observed lower air-sensitivity of $(\eta^5\text{-}C_5H_5)M(\eta^7\text{-}C_7H_7)$ complexes relative to the corresponding $(\eta^6\text{-}C_6H_6)_2M$ complexes.

The theoretical studies on bis(cycloheptatrienyl)metal sandwich complexes in this paper were motivated by the desire to understand the reason for the apparent non-existence of the sandwich compound $(\eta^7\text{-}C_7H_7)_2Ti$ despite the stability of $(\eta^5\text{-}C_5H_5)_2Fe$ and $(\eta^6\text{-}C_6H_6)_2Cr$ (Figure 1). In addition, a variety of $(C_7H_7)_2M$ (M = V to Ni) structures were found with varying hapticity of the C_7H_7 rings guided largely by the 18-electron rule. More surprisingly, the bis(cycloheptatrienyl)chromium sandwich compound $(C_7H_7)_2Cr$ is found to be energetically disfavored with respect to a transannular rearrangement converting a cycloheptatrienyl ring to a tridentate chelating cyclopropyldivinyl ligand. Thus the preferred structure for $(C_7H_7)_2Cr$ is predicted to be a six-coordinate structure of the hexaalkylchromium(VI) type analogous to hexamethyltungsten(VI),[24,25] $(CH_3)_6W$, rather than a bis(cycloheptatrienyl)chromium derivative.

2. Theoretical Methods

Electron-correlation effects were included by employing density functional theory (DFT) methods, which have evolved as a practical and effective computational tool, especially for organometallic compounds.[26–33] Two DFT methods were used in this study. The first functional is the hybrid B3LYP method, which incorporates Becke's three-parameter exchange functional (B3) with the Lee, Yang, and Parr (LYP) correlation functional.[34,35] The second approach is the BP86 method, which marries Becke's 1988 exchange functional (B) with Perdew's 1986 correlation functional.[36,37] It has been noted that the BP86 method may be somewhat more reliable than the B3LYP method for the types of organometallic systems considered in this paper.[38,39]

The geometries of all of the structures were fully optimized using both the DZP B3LYP and DZP BP86 methods. The harmonic vibrational frequencies were determined at the same levels by evaluating analytically the second derivatives of the energy with respect to the nuclear coordinates. The corresponding infrared intensities were evaluated analytically as well. All of the computations were carried out with the Gaussian 03 program in which the fine grid (75,302) is the default for evaluating integrals numerically, and the tight (10^{-8} Hartree) designation is the default for the energy convergence.[40]

For carbon the double-ζ plus polarization (DZP) basis set used here adds one set of pure spherical harmonic d functions with an orbital exponent $\alpha_d(C) = 0.75$ to the standard Huzinaga–Dunning contracted DZ sets, and is designated (9s5p1d/4s2p1d).[41,42] For H, a set of p polarization functions $\alpha_p(H) = 0.75$ is added to the Huzinaga-Dunning DZ sets. For the first-row transition metals, in our loosely contracted DZP basis set, the Wachters' primitive sets are used, but augmented by two sets of p functions and one set of d functions and contracted following Hood et al., and designated (14s11p6d/10s8p3d).[43,44]

In the search for minima, low magnitude imaginary vibrational frequencies are suspect, because the numerical integration procedures used in existing DFT methods have significant limitations.[45] Thus, an imaginary vibrational frequency of magnitude less than 100 $i$cm^{-1} should imply that there is a minimum with energy very similar to that of the stationary point in question. In many cases we do not follow the eigenvectors corresponding to imaginary frequencies less than 100i cm^{-1} in search of another minimum.[46]

3. Results

3.1 Molcular Structures

The geometries of the complexes M(C_7H_7)$_2$ (M = Ti, V, Cr, Mn, Fe, Co, and Ni) were optimized in the lowest electronic singlet and triplet states for Ti, Cr, Fe, and Ni, and the doublet and quartet states for V, Mn, and Co. A sextet state for (C_7H_7)$_2$Mn was also investigated. The stationary

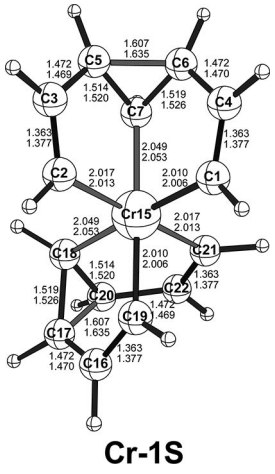

Figure 7. Optimized geometry for the lowest energy Cr(C_7H_7)$_2$ structure.

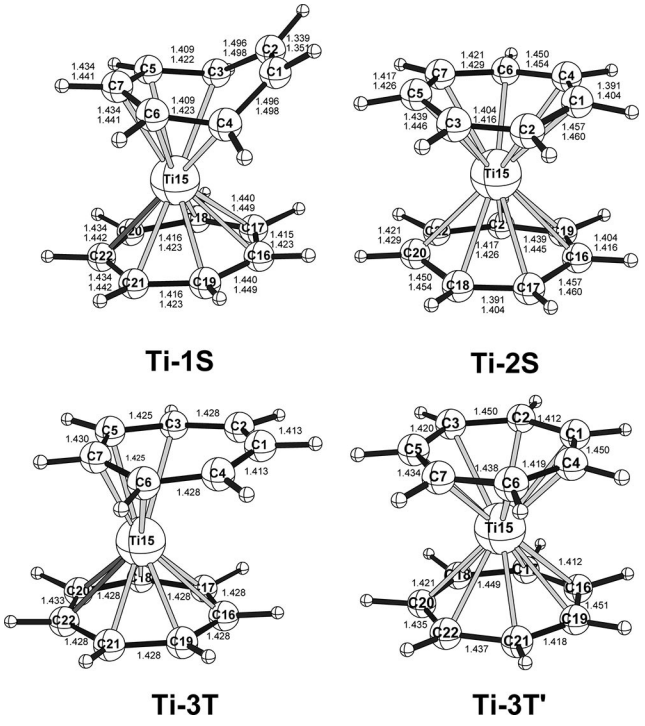

Figure 5. Optimized geometries for the Ti(C_7H_7)$_2$ structures.

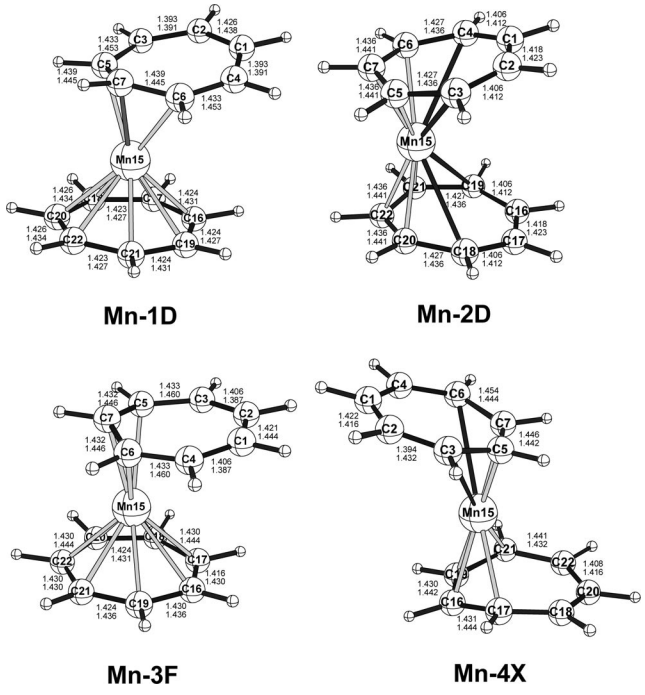

Figure 8. Optimized geometries for the Mn(C_7H_7)$_2$ structures.

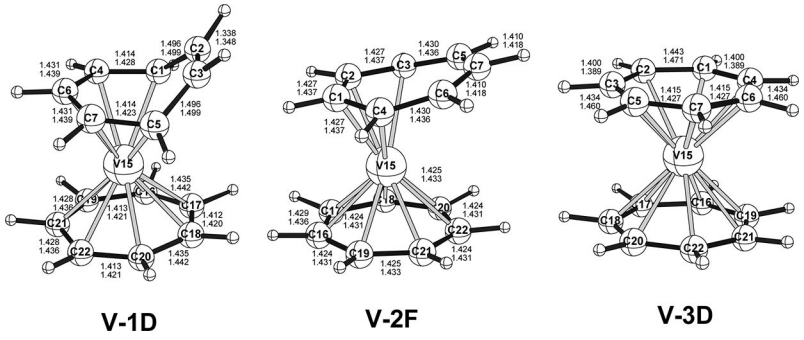

Figure 6. Optimized geometries for the V(C_7H_7)$_2$ structures.

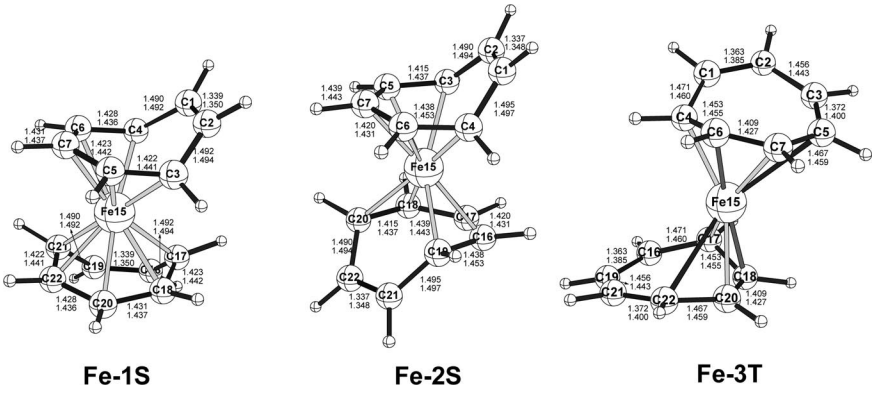

Figure 9. Optimized geometries for the $Fe(C_7H_7)_2$ structures.

point geometries of the energetically low-lying species of $M(C_7H_7)_2$ are shown in Figures 5, 6, 7, 8, 9, 10, and 11, with all C–C bond lengths given in Ångstrøms.

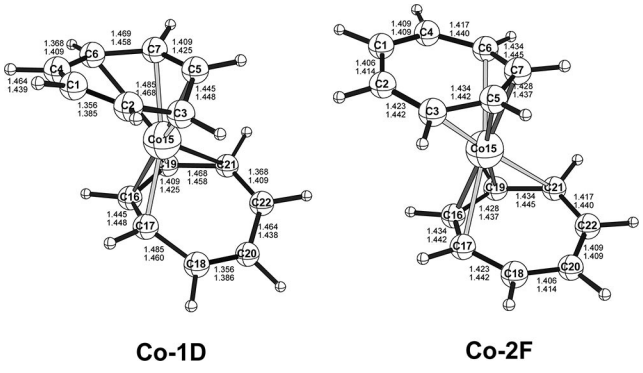

Figure 10. Optimized geometries for the $Co(C_7H_7)_2$ structures.

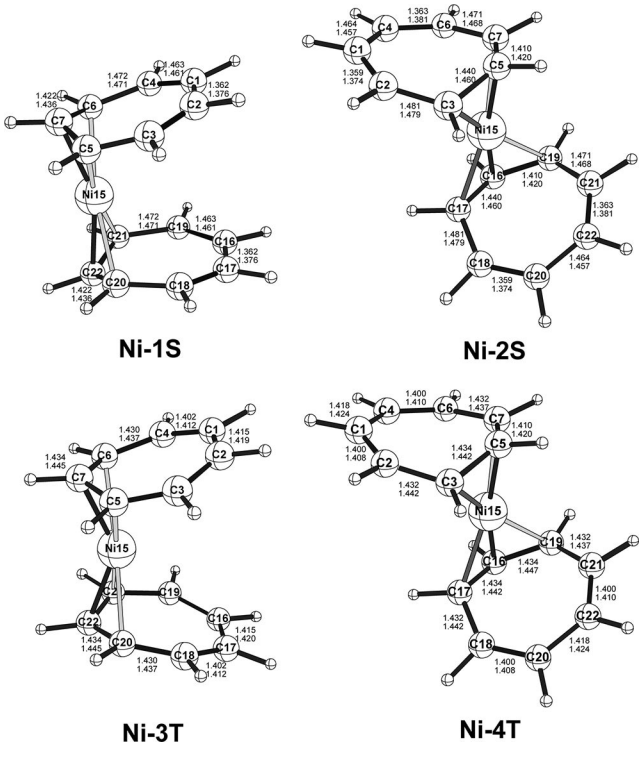

Figure 11. Optimized geometries for the $Ni(C_7H_7)_2$ structures.

3.1.1. Ti(C_7H_7)$_2$

Three energetically low-lying structures were found for $Ti(C_7H_7)_2$ (Figure 5 and Table 1). The global minimum of $Ti(C_7H_7)_2$ (**Ti-1S**) is a singlet (η^7-C_7H_7)Ti(η^5-C_7H_7) structure with one heptahapto and one pentahapto C_7H_7 ring as indicated by the Ti–C distances. The two uncomplexed carbon atoms of the η^5-C_7H_7 ring (C1 and C2 in Figure 5) have Ti–C distances of 3.2 Å. Furthermore, the C=C distance between these carbon atoms is 1.339 Å (B3LYP) or 1.351 Å (BP86), which is appreciably shorter than the other carbon–carbon distances and consistent with an uncomplexed double bond. Structure **Ti-1S** for $(C_7H_7)_2$Ti is thus closely related to the well-known compound[47] (η^7-C_7H_7)$_2$-Ti(η^5-C_5H_5) and has a 16-electron configuration about the titanium atom.

A bis(heptahapto) structure (η^7-C_7H_7)$_2$Ti, namely **Ti-2S** (Figure 5 and Table 1), is also found but at 9.6 kcal/mol (B3LYP) or 5.0 kcal/mol (BP86) above the global minimum **Ti-1S**. More significantly, an imaginary vibrational frequency is found in **Ti-2S** at 49*i* cm^{-1} (B3LYP) or 40*i* cm^{-1} (BP86) for **Ti-2S**. Following the corresponding vibrational mode leads to the global minimum **Ti-1S**. This indicates that the bis(heptahapto) sandwich compound (η^7-C_7H_7)$_2$Ti (**Ti-2S**), having an 18-electron metal configuration analogous to ferrocene and dibenzenechromium (Figure 1), is unstable with respect to the complex (η^7-C_7H_7)Ti-(η^5-C_7H_7) (**Ti-1S**) having two uncomplexed carbon atoms in one of the C_7H_7 rings and only a 16-electron metal configuration.

The lowest lying structure for triplet $(C_7H_7)_2$Ti depends on the DFT method. The B3LYP method predicts a triplet structure (η^7-C_7H_7)Ti(η^4-C_7H_7) (**Ti-3T**), lying 13.2 kcal/mol (B3LYP) above the global minimum. This structure has one heptahapto C_7H_7 ring and one tetrahapto C_7H_7 ring with three carbon atoms not bonded to the metal atom. One of the unpaired electrons in **Ti-3T** (B3LYP) can be delocalized among these three carbon atoms of the η^4-C_7H_7 ring not bonded to the metal atom, leaving the other unpaired electron largely localized on the titanium atom. The BP86 method predicts a bis(heptahapto) (η^7-C_7H_7)$_2$Ti structure **Ti-3T′** as the lowest energy triplet structure lying only 2.4 kcal/mol above the global minimum **Ti-1S**. In the triplet **Ti-3T′** the retention of sevenfold symmetry means

Table 1. Bond lengths [Å], total energies E [Hartree], relative energies ΔE [kcal/mol] and HOMO–LUMO gaps for the $Ti(C_7H_7)_2$ structures.

	Ti-1S (C_s)		**Ti-2S** (C_2)		**Ti-3T** (C_1)	**Ti-3T′** (C_1)
	B3LYP	BP86	B3LYP	BP86	B3LYP	BP86
M–C_7H_7[a]	2.603	2.581	2.352	2.348	2.694	2.360
M–C_7H_7[b]	2.264	2.271	2.352	2.348	2.250	2.360
–HOMO(α)	0.17036	0.15003	0.12835	0.10986	0.14764	0.10599
–LUMO(α)	0.05844	0.09894	0.07070	0.09466	0.06533	0.09699
Gap [eV]	3.05	1.39	1.57	0.41	2.24	0.24
$-E$	1391.42885	1391.54955	1391.41357	1391.54151	1391.40776	1391.54571
ΔE	0.0	0.0	9.6	5.0	13.2	2.4
Imaginary frequency	none	none	49*i*	40*i*	none	43*i*
$\langle S^2 \rangle$	0.00	0.00	0.00	0.00	2.01	2.01

[a] Average M–C_7H_7 upper ring distance. [b] Average M–C_7H_7 lower ring distance (Figure 5).

that the out-of-plane combination of the binodal (δ) ligand π orbitals remains degenerate to accommodate the two unpaired electrons.

3.1.2. $V(C_7H_7)_2$

The structures found for $(C_7H_7)_2V$ (Figure 6 and Table 2) correspond rather closely to the low-energy structures found for $(C_7H_7)_2Ti$. Thus the global minimum of $V(C_7H_7)_2$ is the doublet $(\eta^7\text{-}C_7H_7)V(\eta^5\text{-}C_7H_7)$ (**V-1D** in Figure 6), closely related to the corresponding titanium global minimum $(\eta^7\text{-}C_7H_7)Ti(\eta^5\text{-}C_7H_7)$ (**Ti-1S** in Figure 5) with one heptahapto and one pentahapto C_7H_7 ring. The vanadium structure $(\eta^7\text{-}C_7H_7)V(\eta^5\text{-}C_7H_7)$ (**V-1D**) has a 17-electron metal configuration and is closely related to the compound $(\eta^7\text{-}C_7H_7)_2V(\eta^5\text{-}C_5H_5)$, known since 1959.[9]

The lowest energy quartet structure found for $(C_7H_7)_2V$ is $(\eta^7\text{-}C_7H_7)V(\eta^4\text{-}C_7H_7)$ (**V-2F**) with one heptahapto and one tetrahapto C_7H_7 ring analogous to the lowest energy triplet structure $(\eta^7\text{-}C_7H_7)Ti(\eta^4\text{-}C_7H_7)$ (**Ti-3T**) found for $(C_7H_7)_2Ti$. This quartet structure lies 13.7 kcal/mol (B3LYP) or 13.5 kcal/mol (BP86) above the **V-1D** global minimum.

A higher energy doublet structure **V-3D** (Figure 6) was also found for $(C_7H_7)_2V$ lying 16.3 kcal/mol (B3LYP) or 15.2 kcal/mol (BP86) above the global minimum **V-1D**. This structure is indicated to be a bis(heptahapto) structure by all 14 V–C distances being less than 2.5 Å. However, structure **V-3D** has significant imaginary vibrational frequencies (Table 2), namely 46*i* by B3LYP or 171*i*, 130*i*, 102*i* by BP86. Following the corresponding normal modes of **V-3D** leads to **V-1D** indicating the instability of bis(heptahapto) structures relative to heptahapto-pentahapto structures for vanadium as well as for titanium discussed above.

3.1.3. $Cr(C_7H_7)_2$

The lowest lying singlet structure of $(C_7H_7)_2Cr$ (**Cr-1S** in Figure 7 and Table 3) no longer has intact cycloheptatrienyl rings. Instead the C_7H_7 units are converted to tridentate cyclopropyldivinyl ligands as a result of a cycloheptatrienyl→norcaradienyl rearrangement followed by metal insertion into the carbon–carbon bond opposite the fused three-membered ring. Thus the metallacyclic complex **Cr-1S** may be regarded formally as a hexaalkylchromium derivative with the central chromium atom in the d^0 Cr^{VI} formal oxidation state. The lowest lying triplet structure found for $(C_7H_7)_2Cr$ lies >80 kcal/mol above this singlet bis(cyclopropyldivinyl) Cr^{VI} global minimum **Cr-1S** and thus does not appear to be chemically significant.

Table 3. Bond lengths [Å], total energies E [Hartree], and HOMO–LUMO gap for the lowest lying $Cr(C_7H_7)_2$ structure.

	Cr-1S (C_2)	
	B3LYP	BP86
–HOMO	0.22668	0.19911
–LUMO	0.04451	0.07322
Gap [eV]	4.96	3.43
$-E$	1584.18332	1584.29469
Imaginary frequency	none	none

Table 2. Bond lengths [Å], total energies E [Hartree], relative energies ΔE [kcal/mol] and HOMO–LUMO gaps for the $V(C_7H_7)_2$ structures.

	V-1D (C_s)		**V-2F** (C_s)		**V-3D** (C_{2v})	
	B3LYP	BP86	B3LYP	BP86	B3LYP	BP86
V–C_7H_7[a]	2.545	2.522	2.671	2.615	2.316	2.350
V–C_7H_7[b]	2.235	2.233	2.222	2.230	2.316	2.350
–HOMO(α)	0.17456	0.14061	0.14584	0.12570	0.12125	0.11404
–LUMO(α)	0.04930	0.07678	0.02905	0.05736	0.06941	0.09218
Gap [eV]	3.41	1.74	3.18	1.86	1.41	0.59
$-E$	1485.96019	1486.10586	1485.93830	1486.08437	1485.93416	1486.08164
ΔE	0.0	0.0	13.7	13.5	16.3	15.2
Imaginary frequency	none	none	none	none	46*i*	171*i*, 130*i*, 102*i*
$\langle S^2 \rangle$	0.82	0.78	3.83	3.78	0.78	0.79

[a] Average M–C_7H_7 upper ring distance. [b] Average M–C_7H_7 lower ring distance (Figure 6).

3.1.4. $Mn(C_7H_7)_2$

Four low-lying structures (two doublets, one quartet, and one sextet) were found for $Mn(C_7H_7)_2$ (Figure 8 and Table 4). The global minimum **Mn-1D** is predicted to be a doublet having a structure (η^7-C_7H_7)Mn(η^3-C_7H_7) with one heptahapto and one trihapto C_7H_7 ring leading to a 17-electron metal configuration. Two of the C=C distances in the chain of four uncomplexed carbon atoms in the η^3-C_7H_7 ring of **Mn-1D** are 1.39 Å (Figure 8) corresponding to double bonds in a *cis* butadienoid unit.

A second doublet structure **Mn-2D** for $Mn(C_7H_7)_2$ was found to lie 9.2 kcal/mol (B3LYP) or 19.7 kcal/mol (BP86) above this global minimum. However, this structure has two or three imaginary vibrational frequencies (Table 4). Following the largest imaginary frequency of **Mn-2D** leads to the global minimum **Mn-1D**.

The lowest lying quartet structure of $(C_7H_7)_2Mn$ is a heptahapto-trihapto derivative (η^7-C_7H_7)Mn(η^3-C_7H_7) (**Mn-3F**) lying 5.3 kcal/mol (B3LYP) or 24.9 kcal/mol (BP86) above the doublet global minimum **Mn-1D**. Relatively large spin contamination (based on the use of the DFT orbitals in a single determinant wave function) is found in the $Mn(C_7H_7)_2$ structures calculated by the B3LYP method. This tends to confirm the view that the BP86 predictions are more reliable than the B3LYP predictions.[38,39]

In view of this significant spin contamination for the quartet structure **Mn-3F**, particularly using the B3LYP method, calculations were also done on sextet structures of $(C_7H_7)_2Mn$ noting that bis(cyclopentadienyl)manganese, $(C_5H_5)_2Mn$, is a sextet corresponding to the five unpaired electrons of the half-filled d^5 shell of Mn^{II}.[48] However, the lowest lying sextet structure, namely **Mn-4X** (Figure 8 and Table 4), was found to lie at the relatively high energy of 18.1 kcal/mol (B3LYP) or 32.6 kcal/mol (BP86) above the global minimum **Mn-1D**. The Mn–C distances in **Mn-4X** suggest a (η^4-C_7H_7)$_2$Mn structure with two tetrahapto C_7H_7 rings. Since the η^4-C_7H_7 rings can be regarded as neutral free radical ligands, (η^4-C_7H_7)$_2$Mn (**Mn-4X**) is not a formal sextet d^5 Mn^{II} derivative but instead a formal quartet d^7 Mn(0) derivative with the extra two unpaired electrons on the C_7H_7 ligands. This may account for the relatively high energy of **Mn-4X**. Thus (η^4-C_7H_7)$_2$Mn (**Mn-4X**) is not at all analogous to $(C_5H_5)_2Mn$.

3.1.5. $Fe(C_7H_7)_2$

Both of the stationary points found for singlet $Fe(C_7H_7)_2$ (Figure 9 and Table 5) are bis(pentahapto) structures (η^5-C_7H_7)$_2$Fe, differing only in the relative positions of the two uncomplexed C=C double bonds on the two rings. The *trans* structure **Fe-2S** lies 5.7 kcal/mol (B3LYP) or 5.3 kcal/mol (BP86) above the global minimum *cis* structure **Fe-1S**. The closeness in the energies of these two (η^5-C_7H_7)$_2$Fe structures suggests a highly fluxional system.

The lowest energy triplet structure **Fe-3T** is a bis(tetrahapto)structure (η^4-C_7H_7)$_2$Fe 4.4 kcal/mol (B3LYP) or 18.1 kcal/mol (BP86) above the global minimum singlet structure **Fe-1S**. In **Fe-3T** the two unpaired electrons of the triplet can be considered to be largely localized in each uncomplexed allylic unit of the tetrahapto η^4-C_7H_7 rings.

Table 4. Bond lengths [Å], total energies E [Hartree], relative energies ΔE [kcal/mol] and HOMO–LUMO gaps for the $Mn(C_7H_7)_2$ structures.

	Mn-1D (C_s)		**Mn-2D** (C_{2v})		**Mn-3F** (C_1)		**Mn-4X**	
	B3LYP	BP86	B3LYP	BP86	B3LYP	BP86	B3LYP (C_s)	BP86(C_{2h})
Mn–C_7H_7[a]	2.879	2.823	2.666	2.533	3.117	2.770	2.924	2.604
Mn–C_7H_7[b]	2.278	2.178	2.666	2.533	2.286	2.276	2.613	2.604
–HOMO(α)	0.20093	0.15228	0.20870	0.15456	0.13040	0.10605	0.14057	0.12100
–LUMO(α)	0.06723	0.07986	0.08283	0.10138	0.07367	0.08489	0.06810	0.07780
Gap [eV]	3.64	1.97	3.43	1.45	1.54	0.58	1.97	1.18
$-E$	1692.92268	1693.11555	1692.90796	1693.08407	1692.91417	1693.07587	1692.89376	1693.06354
ΔE	0.0	0.0	9.2	19.7	5.3	24.9	18.1	32.6
Imaginary frequency	17*i*	none	75*i*, 45*i*	122*i*, 83*i*, 58*i*	none	none	none	none
$\langle S^2 \rangle$	2.63	0.89	3.20	1.27	5.20	4.00	9.48	8.85

[a] Average M–C_7H_7 upper ring distance. [b] Average M–C_7H_7 lower ring distance (Figure 8).

Table 5. Bond lengths [Å], total energies E [Hartree], relative energies ΔE [kcal/mol], and HOMO–LUMO gap for the $Fe(C_7H_7)_2$ structures.

	Fe-1S (C_2)		**Fe-2S** (C_2)		**Fe-3T** (C_2)	
	B3LYP	BP86	B3LYP	BP86	B3LYP	BP86
Fe–C_7H_7[a]	2.359	2.344	2.372	2.355	2.683	2.582
Fe–C_7H_7[b]	2.359	2.344	2.372	2.355	2.683	2.582
–HOMO(α)	0.17670	0.15780	0.18758	0.15354	0.15240	0.12834
–LUMO(α)	0.03140	0.06430	0.02538	0.06374	0.07142	0.10014
Gap [eV]	3.95	2.54	4.41	2.44	2.20	0.77
$-E$	1805.62931	1805.85201	1805.62025	1805.84358	1805.62224	1805.82313
ΔE	0.0	0.0	5.7	5.3	4.4	18.1
Imaginary frequency	none	none	none	none	none	none
$\langle S^2 \rangle$	0.00	0.00	0.00	0.00	2.22	2.12

[a] Average M–C_7H_7 upper ring distance. [b] Average M–C_7H_7 lower ring distance (Figure 9).

3.1.6. $Co(C_7H_7)_2$

The global minimum **Co-1D** for $Co(C_7H_7)_2$ (Figure 10 and Table 6) may be regarded as a *trans* bis(trihapto) structure $(\eta^3\text{-}C_7H_7)_2Co$. The cobalt atom thus has only a 15-electron configuration. The four carbons of each $\eta^3\text{-}C_7H_7$ ligand not bonded to the cobalt atom (i.e., with Co–C distances > 2.3 Å) form a *cis*-diene unit with C=C bond lengths in the range 1.35 to 1.41 Å. However, one of the four carbons of the *cis*-diene unit of each $\eta^3\text{-}C_7H_7$ ring in **Co-1D** is at an intermediate distance from the cobalt atom (2.25 Å by B3LYP or 2.57 Å by BP86), suggesting an additional weaker Co–C interaction. This is consistent with the electron deficiency of the formally 15-electron cobalt atom in a $(\eta^3\text{-}C_7H_7)_2Co$ structure.

The lowest energy quartet structure **Co-2F** for $Co(C_7H_7)_2$ is a bis(tetrahapto) structure $(\eta^4\text{-}C_7H_7)_2Co$ (Figure 10 and Table 6) lying 16.3 kcal/mol (B3LYP) or 14.4 kcal/mol (BP86) above the doublet global minimum **Co-1D**. The cobalt atom has a 17-electron configuration suggesting that one of the three unpaired electrons in the quartet **Co-2F** is localized on the cobalt atom and the other two unpaired electrons are localized on the uncomplexed allylic units in the $\eta^4\text{-}C_7H_7$ rings.

Table 6. Bond lengths [Å], total energies E [Hartree], relative energies ΔE [kcal/mol] and HOMO–LUMO gaps for the $Co(C_7H_7)_2$ structures.

	Co-1D (C_2)		**Co-2F** (C_2)	
	B3LYP	BP86	B3LYP	BP86
Co–C_7H_7[a]	2.619	2.533	2.627	2.554
Co–C_7H_7[b]	2.619	2.533	2.627	2.554
–HOMO(α)	0.15865	0.12935	0.13663	0.12391
–LUMO(α)	0.06665	0.10099	0.05851	0.07633
Gap [eV]	2.50	0.77	2.13	1.29
$-E$	1924.70036	1924.91909	1924.67432	1924.89610
ΔE	0.0	0.0	16.3	14.4
Imaginary frequency	none	none	none	none
$\langle S^2 \rangle$	0.81	0.77	3.76	3.76

[a] Average M–C_7H_7 upper ring distance. [b] Average M–C_7H_7 lower ring distance (Figure 10).

3.1.7. $Ni(C_7H_7)_2$

Four structures for $Ni(C_7H_7)_2$ were found (Figure 11 and Table 7). Two of these structures are singlets and two are triplets. None of these $(C_7H_7)_2Ni$ structures has any imaginary vibrational frequencies. All of these $(C_7H_7)_2Ni$ structures are of the type $(\eta^3\text{-}C_7H_7)_2Ni$ with two trihapto C_7H_7 ligands as clearly indicated by their Ni–C distances. The singlet *cis* structure **Ni-1S** is the global minimum. However, the corresponding *trans* structure **Ni-2S** lies within 1 kcal/mol of this global minimum, suggesting a potentially fluxional system. The nickel atoms in both **Ni-1S** and **Ni-2S** have 16-electron configurations with a nickel environment very similar to the well-known[49] bis(η^3-allyl)nickel, $(\eta^3\text{-}C_3H_5)_2Ni$. The two triplet structures **Ni-3T** and **Ni-4T** found for $(C_7H_7)_2Ni$ have similar $\eta^3\text{-}C_7H_7Ni$ local geometries to the corresponding singlet structures **Ni-1S** and **Ni-2S**, respectively. However, both triplet structures lie more than 11 kcal/mol above the singlet global minimum **Ni-1S**.

3.2. Charge Distributions

The partial charges on the upper C_7H_7 ring, metal atom, and the lower C_7H_7 ring (as depicted in the Figures) were obtained by a Mulliken population analysis (Table 8). The total dipole moments are also shown in Table 8. The charge distributions found using the B3LYP method are consistently larger than those found using the BP86 method. The largest dipole moment and "charge" at the metal atom among all of the $(C_7H_7)_2M$ derivatives is found in $(\eta^7\text{-}C_7H_7)Mn(\eta^3\text{-}C_7H_7)$ (**Mn-1D** in Figure 8) with one heptahapto and one trihapto C_7H_7 ring. The electron distributions found for each member of the stereoisomer pairs $(\eta^5\text{-}C_7H_7)_2Fe$ **Fe-1S** and **Fe-2S** and $\eta^3\text{-}(C_7H_7)_2Ni$ (**Ni-1S** and **Ni-2S**) are essentially identical. The NBO atomic charges are smaller than the formal charges.

3.3. Orbital Analysis

Orbital analyses were performed for the lowest energy $M(C_7H_7)_2$ structures. The schematic qualitative energy level diagrams for the frontier MOs of the most stable structures with the BP86 method are displayed in Figure 12. The largest HOMO–LUMO energy gap (3.43 eV) is found for $Cr(C_7H_7)_2$ (**Cr-1S** in Figure 7) in which the C_7H_7 ring has rearranged to a tridentate cyclopropyldivinyl ligand and the chromium atom is in the d^0 +6 formal oxidation state. In a $(C_7H_7)_2M$ derivative with an intact cycloheptatrienyl ring

Table 7. Bond lengths [Å], total energies *E* [Hartree], relative energies Δ*E* [kcal/mol] and HOMO–LUMO gap for the $Ni(C_7H_7)_2$ structures.

	Ni-1S (C_{2v})		**Ni-2S** (C_2)		**Ni-3T** (C_{2v})		**Ni-4T** (C_2)	
	B3LYP	BP86	B3LYP	BP86	B3LYP	BP86	B3LYP	BP86
Ni–C_7H_7[a]	2.692	2.694	2.680	2.662	2.700	2.675	2.710	2.700
Ni–C_7H_7[b]	2.692	2.694	2.680	2.663	2.700	2.675	2.710	2.700
–HOMO(α)	0.155549	0.13853	0.15701	0.14202	0.12879	0.11820	0.13337	0.12264
–LUMO(α)	0.07197	0.10184	0.07304	0.10040	0.06674	0.08735	0.06816	0.08958
Gap/eV	2.27	1.00	2.28	1.13	1.69	0.84	1.77	0.90
$-E$	2050.26198	2050.49502	2050.26229	2050.49376	2050.23721	2050.47644	2050.24213	2050.47714
ΔE	0.0	0.0	0.2	0.8	15.5	11.7	12.5	11.2
Imaginary frequency	none	none	none	none	none	none	19*i*	none
$\langle S^2 \rangle$	0.00	0.00	0.00	0.00	2.08	2.00	2.12	2.01

[a] Average M–C_7H_7 upper ring distance. [b] Average M–C_7H_7 lower ring distance (Figure 11).

Table 8. Partial charges on the C_7H_7 rings and the metal atom; total dipole moment in Debye.

	Upper C_7H_7 ring		Metal		Lower C_7H_7 ring		Dipole moment	
	B3LYP	BP86	B3LYP	BP86	B3LYP	BP86	B3LYP	BP86
Ti-1S	–0.15	–0.15	0.45	0.42	–0.30	–0.27	1.38	1.28
Ti-2S	–0.17	–0.15	0.33	0.31	–0.17	–0.15	0.09	0.09
Ti-3T	–0.21	–0.14	0.55	0.28	–0.35	–0.14	0.84	0.04
V-1D	–0.23	–0.21	0.37	0.31	–0.14	–0.10	1.06	1.04
V-2F	–0.29	–0.26	0.47	0.42	–0.18	–0.16	0.46	0.38
Cr-1S	–0.01	0.06	0.03	–0.13	–0.01	0.06	0.78	0.83
Mn-1D	–0.27	–0.20	0.54	0.39	–0.27	–0.19	2.06	2.04
Mn-2D	–0.29	–0.25	0.59	0.49	–0.29	–0.25	1.01	0.68
Mn-3F	–0.24	–0.30	0.58	0.46	–0.34	–0.15	2.68	0.37
Fe-1S	–0.16	–0.11	0.32	0.21	–0.16	–0.11	1.46	1.39
Fe-2S	–0.17	–0.11	0.34	0.22	–0.17	–0.11	0.69	0.63
Fe-3T	–0.23	–0.19	0.46	0.38	–0.23	–0.19	1.11	0.75
Co-1D	–0.19	–0.15	0.39	0.29	–0.19	–0.15	0.91	0.60
Co-2F	–0.16	–0.15	0.32	0.30	–0.16	–0.15	0.09	0.25
Ni-1S	–0.16	–0.15	0.33	0.30	–0.16	–0.15	0.79	0.70
Ni-2S	–0.16	–0.15	0.32	0.29	–0.16	–0.15	0.51	0.77
Ni-3T	–0.17	–0.16	0.34	0.33	–0.17	–0.16	0.77	0.72
Ni-4T	–0.14	–0.12	0.28	0.25	–0.14	–0.12	0.00	0.12

the largest HOMO–LUMO energy gap, namely 2.54 eV, is found in $(\eta^5\text{-}C_7H_7)_2Fe$ (**Fe-1S** in Figure 9), which is closely related to the very stable ferrocene (Figure 1).

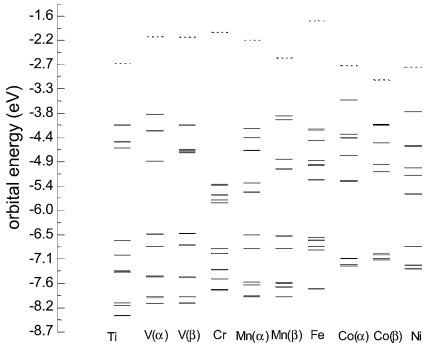

Figure 12. Energies of the frontier MOs of the lowest energy $M(C_7H_7)_2$ structures. Bonding MOs are solid lines whereas the LUMOs are dotted lines.

Figure 13 and Figure 14 compare the frontier molecular orbitals (LUMO down to HOMO–6) for the sandwich compound $(\eta^7\text{-}C_7H_7)_2Ti$ (Figure 1 and **Ti-2S** in Figure 5) and the $(\eta^7\text{-}C_7H_7)Ti(\eta^5\text{-}C_7H_7)$ global minimum (**Ti-1S** in Figure 5), which has one pentahapto C_7H_7 ring and an uncomplexed C=C double bond. For the high symmetry sandwich compound $(\eta^7\text{-}C_7H_7)_2Ti$ **Ti-2S** (Figure 13) the five highest lying filled molecular orbitals (HOMO to HOMO–4) represent the interactions of the five titanium d orbitals with the C_7H_7 rings. The LUMO, HOMO–5 and HOMO–6 orbitals are localized purely on the C_7H_7 rings. Thus the HOMO for $(\eta^7\text{-}C_7H_7)_2Ti$ corresponds to the σ interaction of the titanium d_{z^2} orbital with the C_7H_7 ring orbitals of suitable symmetry. The next two orbitals, HOMO–1 and HOMO–2, correspond to the δ interactions of the $d_{x^2-y^2}$ and d_{xy} orbitals with the corresponding C_7H_7 ring orbitals. Then come the HOMO–3 and HOMO–4 corresponding to the π interactions of the d_{xz} and d_{yz} orbitals with the corresponding C_7H_7 ring orbitals. The 18-electron titanium configuration of $(\eta^7\text{-}C_7H_7)_2Ti$ (Figure 1 and **Ti-2S** in Figure 5) may be viewed (in a simple picture) as arising from the filling of the nine-orbital sp^3d^5 manifold.

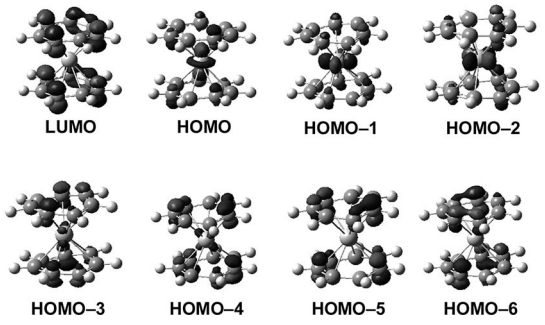

Figure 13. The frontier orbitals for $(\eta^7\text{-}C_7H_7)_2Ti$ (**Ti-2S** in Figure 5).

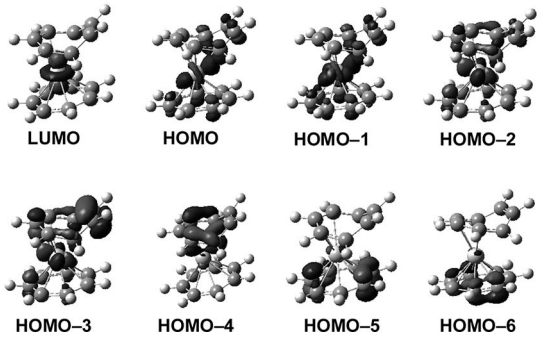

Figure 14. The frontier orbitals for $(\eta^7\text{-}C_7H_7)Ti(\eta^5\text{-}C_7H_7)$ (**Ti-1S** in Figure 5).

Comparison of Figure 14 with Figure 13 shows the effect on the frontier molecular orbitals accompanying distortion of $(\eta^7\text{-}C_7H_7)_2Ti$ (**Ti-2S** in Figure 5) to the $(\eta^7\text{-}C_7H_7)Ti(\eta^5\text{-}C_7H_7)$ global minimum (**Ti-1S** in Figure 5). The five metal d orbitals and their interactions with C_7H_7 ring orbitals of suitable symmetry now correspond to LUMO and HOMO

to HOMO–3. Going from an 18-electron titanium configuration in $(\eta^7\text{-}C_7H_7)_2Ti$ to a 16-electron titanium configuration in $(\eta^7\text{-}C_7H_7)Ti(\eta^5\text{-}C_7H_7)$ is seen to involve transfer of a pair of electrons from the titanium d_{z^2} orbital to a lower lying bonding MO corresponding to the uncomplexed C=C double bond in the $\eta^5\text{-}C_7H_7$ ring. This is seen (Figure 13 and Figure 14) by the HOMO titanium d_{z^2} orbital and its relatively weak metal–ring interactions in $(\eta^7\text{-}C_7H_7)_2Ti$ (Figure 13) becoming the LUMO in $(\eta^7\text{-}C_7H_7)Ti(\eta^5\text{-}C_7H_7)$ (Figure 14) corresponding to a "pure" titanium d_{z^2} orbital with no apparent interaction with the ring orbitals. Thus the 16-electron configuration of the titanium atom in $(\eta^7\text{-}C_7H_7)Ti(\eta^5\text{-}C_7H_7)$ (**Ti-1S** in Figure 5) is seen at least formally to arise by emptying the d_{z^2} orbital and thus corresponds to a filled $sp^3d^4(xz, yz, xy, x^2–y^2)$ eight-orbital manifold rather than the filled nine-orbital sp^3d^5 manifold of $(\eta^7\text{-}C_7H_7)_2Ti$. We must emphasize that such valence bond metal descriptions should not be taken literally, as there is no ab initio evidence for the required high 4p orbital occupations.

4. Discussion

Figure 15 shows five ways that a cycloheptatrienyl ring can bond through a transition metal using from three to all seven of its carbon atoms. These bonding modes have the following features.

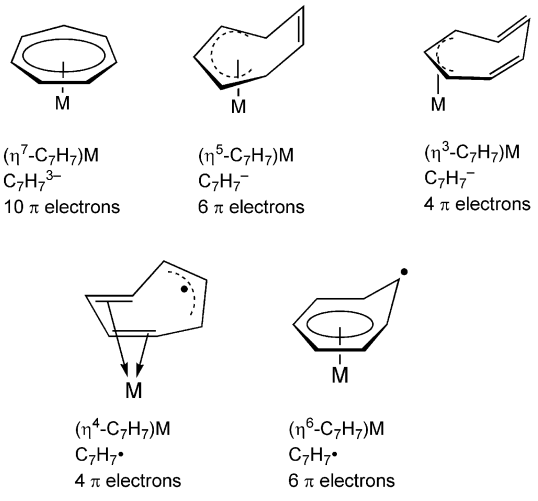

Figure 15. Five ways of bonding a cycloheptatrienyl (C_7H_7) ligand to a metal atom.

(1) Heptahapto $\eta^7\text{-}C_7H_7$ Bonding Using All Seven Carbon Atoms: The C_7H_7 ligand in such complexes can be considered formally to be the $C_7H_7^{3-}$ trianion with 10 π-electrons in accord with the Hückel $4n + 2$ π-electron rule for planar cyclic aromatic systems. The bonding of an $\eta^7\text{-}C_7H_7$ ligand to the metal atom has five components: one σ component using metal s, p_z, and/or d_{z^2} orbitals, two π components using p_x and p_y as well as d_{xz} and d_{yz} orbitals, and two δ components using $d_{x^2–y^2}$ and d_{xy} orbitals (assuming that the C_7 axis of the C_7H_7 ring is the z axis).

(2) Pentahapto $\eta^5\text{-}C_7H_7$ Bonding Using Five Carbon Atoms Leaving an Uncomplexed C=C Double Bond: The C_7H_7 ligand in such complexes can be considered formally to be the $C_7H_7^-$ monoanion with 6 π electrons involved in the bonding to the metal atom. The bonding of an $\eta^5\text{-}C_7H_7$ ligand to the metal atom has three components, namely one σ component and two π components using the same metal orbitals as for the corresponding metal–ring bonds in the $\eta^7\text{-}C_7H_7$ metal complexes discussed above. The uncomplexed C=C double bond in a $\eta^5\text{-}C_7H_7$ ligand is unusually short compared with the carbon–carbon bonds involving the carbons bonded to the metal atom.

(3) Trihapto $\eta^3\text{-}C_7H_7$ Bonding Using Three Carbon Atoms Leaving an Uncomplexed *cis*-1,3-Butadiene Unit: The $\eta^3\text{-}C_7H_7$ ligand in such complexes is closely related to the trihaptoallyl ligand and can be considered formally to be a monoanion with 4 π electrons similar to the allyl anion. The bonding of a $\eta^3\text{-}C_7H_7$ ligand to a metal atom, like that of a $\eta^3\text{-}C_3H_5$ ligand, can be considered to consist of one σ and one π bond. The $\eta^3\text{-}C_7H_7$ ligand contains an uncomplexed *cis*-1,3-butadiene unit, as indicated by its carbon–carbon bond lengths.

(4) Tetrahapto $\eta^4\text{-}C_7H_7$ Bonding Using Four Carbon Atoms Leaving an Unpaired Electron on the Allylic Unit Not Bonded to the Metal Atom: This ligand resembles a tetrahapto *cis* butadiene ligand and is predicted to occur in some triplet and quartet structures found in this work including **Ti-3T** (Figure 5), **V-3F** (Figure 6), **Fe-3T** (Figure 9), and **Co-2F** (Figure 10) as well as the sextet structure **Mn-4X** (Figure 8).

(5) Hexahapto $\eta^6\text{-}C_7H_7$ Bonding Using Six Carbon Atoms Leaving an Unpaired Electron on the Carbon Not Bonded to the Metal Atom: No examples of hexahapto C_7H_7 ligands were found in this work. However, the hypothetical $(\eta^6\text{-}C_7H_7)_2Cr$ complex might be an intermediate to the formation of the bis(tridentate) cyclopropyldivinyl Cr^{VI} derivative **Cr-1S** (Figure 7).

One of the major conclusions from this theoretical study is that the bis(heptahapto) sandwich compound $(\eta^7\text{-}C_7H_7)_2Ti$ is not likely to be a viable species unlike dibenzenechromium and ferrocene (Figure 1). Simple analyses suggest instability of the titanium sandwich $(\eta^7\text{-}C_7H_7)_2Ti$ for the following reasons:

(1) The presence of two $\eta^7\text{-}C_7H_7$ 10 π-electron rings on a titanium atom with their –3 formal charges gives the central titanium atom a +6 formal oxidation state. Such a high titanium oxidation state, even if only formal, is clearly unreasonable since it requires loss of two electrons from an inner electron shell in addition to loss of all four electrons in the titanium valence shell.

(2) Each $\eta^7\text{-}C_7H_7$–Ti bond with its five components ($\sigma + 2\pi + 2\delta$) requires five metal orbitals implying the need for ten orbitals for a $(\eta^7\text{-}C_7H_7)_2Ti$ structure. However, there are only nine orbitals in the accessible sp^3d^5 valence orbital manifold for titanium suggesting the impossibility (or at least unfavorability) of bis(heptahapto) bonding. However, for actinides, with f orbitals available in the valence shell, $(\eta^7\text{-}C_7H_7)_2M$ derivatives with two heptahapto C_7H_7 rings

are feasible as indicated by the synthesis of the anion $(\eta^7\text{-}C_7H_7)_2U^-$ by Ephritikhine and co-workers.[50]

The present results support the unlikelihood of a bis(heptahapto) structure for $(\eta^7\text{-}C_7H_7)_2Ti$ in the following two ways:

(1) A heptahapto-pentahapto structure $(\eta^7\text{-}C_7H_7)Ti(\eta^5\text{-}C_7H_7)$ (**Ti-1S** in Figure 5) is found for $(C_7H_7)_2Ti$ of significantly lower energy than the bis(heptahapto) structure.

(2) The higher energy bis(heptahapto) structure $(\eta^7\text{-}C_7H_7)_2Ti$ (**Ti-2S** in Figure 5) has a $40\,i\,cm^{-1}$ imaginary vibrational frequency. Following the corresponding normal mode leads to the lower energy $(\eta^7\text{-}C_7H_7)Ti(\eta^5\text{-}C_7H_7)$ (**Ti-1S**) structure. Thus the bis(heptahapto) structure $(\eta^7\text{-}C_7H_7)_2Ti$ is a transition state rather than a true minimum.

The lowest lying structures for $(C_7H_7)_2M$ (M = Ti, V) are the heptahapto-pentahapto structures $(\eta^7\text{-}C_7H_7)M(\eta^5\text{-}C_7H_7)$. However, an analogous structure is not found at a competitive energy for $(C_7H_7)_2Cr$. Instead the lowest energy structure **Cr-1S** for $(C_7H_7)_2Cr$ (Figure 7) has two chelating tridentate cyclopropyldivinyl ligands formed by rearrangement of the cycloheptatrienyl rings. The resulting formally chromium(VI) hexaalkyl can arise from a bis(hexahaptocycloheptatrienyl)chromium derivative $(\eta^6\text{-}C_7H_7)_2Cr$ through a pentahapto norcaradienyl intermediate (Figure 16) in which the norcaradienyl ligand is linked to the chromium atom through its two double bonds as well as a Cr–alkyl bond to the cyclopropyl carbon not bearing a vinyl group. A simple rearrangement of this η^5-norcaradienyl ligand can then lead to the observed tridentate chelating cyclopropyldivinyl ligand

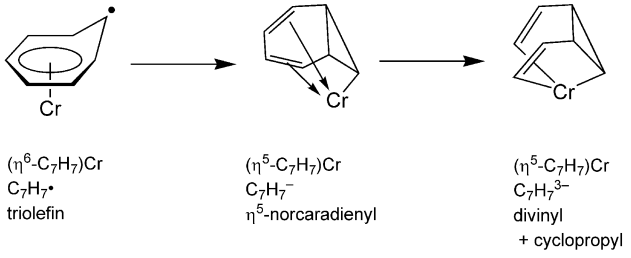

Figure 16. A possible mechanism for the rearrangement of a $(\eta^6\text{-}C_7H_7)Cr$ structure to the tridentate chelating cyclopropylbis(divinyl) structure. For clarity only one of the C_7H_7 ligands is shown.

The lowest energy $(C_7H_7)_2M$ structures for the later first-row transition metals from manganese to nickel have cycloheptatrienyl rings partially bonded to the metal atom through pentahapto and trihapto bonding. In general structures with the lowest spin multiplicity have the lowest energies. Thus the lowest energy structures for the iron and nickel derivatives are singlets and those for the manganese and cobalt derivatives are doublets. For iron, the lowest energy structures are the singlet *cis* and *trans* pentahapto $(\eta^5\text{-}C_7H_7)_2Fe$ derivatives (**Fe-1S** and **Fe-2S** in Figure 9), which are of similar energies with an 18-electron local iron environment and a metal formal oxidation state of +2 very similar to that in ferrocene. For nickel, the lowest energy structures are the singlet *cis* and *trans* stereoisomers of trihapto $(\eta^3\text{-}C_7H_7)_2Ni$ (**Ni-1S** and **Ni-2S** in Figure 11) with a local nickel environment very similar to that in bis(η^3-allyl)nickel and again a metal formal oxidation state of +2. For manganese, the doublet heptahapto-trihapto structure $(\eta^7\text{-}C_7H_7)Mn(\eta^3\text{-}C_7H_7)$ (**Mn-1D** in Figure 8) is of lower energy than the more symmetrical doublet bis(pentahapto) structure $(\eta^5\text{-}C_7H_7)_2Mn$ (**Mn-2D**). The lowest energy structure for $(C_7H_7)_2Co$ is a bis(trihapto) structure (**Co-1D**) with a 15-electron metal configuration.

None of the $(C_7H_7)_2M$ derivatives predicted in this paper has been synthesized to date. A possible synthetic method might involve reactions of the $C_7H_7^{3-}$ trianion with suitable metal halides or other related metal derivatives. A possible source of the required trianion is the metallation of 1,4-cycloheptadiene with suitable organolithium derivatives.[22] However, at the present time this does not seem to be a particularly clean reaction so improvements in the cycloheptadiene metallation procedure might be necessary before this synthetic method can be used.

Supporting Information (see also the footnote on the first page of this article): Complete tables of metal–carbon distances [Å] for the $M(C_7H_7)_2$ (M = Ti, V, Mn, Fe, Co, Ni) structures (Tables S1 to S6); complete tables of vibrational frequencies for $(C_7H_7)_2M$ (M = Ti, V, Cr, Mn, Fe, Co, Ni) structures (Tables S7 to S25); coordinates of the $(C_7H_7)_2M$ (M = Ti, V, Cr, Mn, Fe, Co, Ni) structures (Tables S26 to S43).

Acknowledgments

We are grateful to the Chinese National Science Foundation (Grants 10774104) and the U. S. National Science Foundation (Grant CHE-0209857, CHE-0716718, and CHE-074986) for support of this work.

[1] T. J. Kealy, P. L. Pauson, *Nature* **1951**, *168*, 1039.
[2] S. A. Miller, J. A. Tebboth, J. F. Tremaine, *J. Chem. Soc.* **1952**, 632.
[3] E. O. Fischer, W. Hafner, *Z. Naturforsch., Teil B* **1955**, *10*, 665.
[4] M. T. Anthony, M. L. H. Green, D. Young, *J. Chem. Soc., Dalton Trans.* **1975**, 1419.
[5] O. N. Krasochka, A. F. Shestakov, G. G. Tairova, Yu. A. Shvetsov, E. F. Kvashina, V. I. Onomarev, L. O. Atovmyan, Yu. G. Borod'ko, *Khim. Fiz.* **1983**, *2*, 1459.
[6] M. L. H. Green, D. K. P. Ng, *Chem. Rev.* **1995**, *95*, 439.
[7] H. J. Dauben Jr, L. R. Honnen, *J. Am. Chem. Soc.* **1958**, *80*, 5570.
[8] G. R. Clark, G. Palenik, *J. Organomet. Chem.* **1973**, *50*, 185.
[9] R. B. King, F. G. A. Stone, *J. Am. Chem. Soc.* **1959**, *81*, 5263.
[10] G. Engebretson, R. E. Rundle, *J. Am. Chem. Soc.* **1963**, *85*, 481.
[11] R. B. King, M. B. Bisnette, *Tetrahedron Lett.* **1963**, *4*, 1137.
[12] R. B. King, M. B. Bisnette, *Inorg. Chem.* **1964**, *3*, 785.
[13] J. W. Faller, *Inorg. Chem.* **1969**, *8*, 767.
[14] T. H. Whitesides, R. A. Budnik, *Inorg. Chem.* **1976**, *15*, 874.
[15] D. M. Heinekey, W. A. G. Graham, *J. Am. Chem. Soc.* **1979**, *101*, 6115.
[16] D. M. Heinekey, W. A. G. Graham, *J. Organomet. Chem.* **1982**, *232*, 335.
[17] E. W. Abel, M. A. Bennett, R. Burton, G. Wilkinson, *J. Chem. Soc.* **1958**, 4559.
[18] C. E. Davies, I. M. Gardiner, J. C. Green, M. L. H. Green, N. J. Hazel, P. D. Grebenik, V. S. B. Mtetwa, K. Prout, *J. Chem. Soc., Dalton Trans.* **1985**, 669.

[19] J. C. Green, M. L. H. Green, N. Kaltsoyannis, P. Mountford, P. Scott, S. J. Simpson, *Organometallics* **1992**, *11*, 3353.
[20] G. Menconi, N. Kaltsoyannis, *Organometallics* **2005**, *24*, 1459.
[21] M. Tamm, A. Kunst, T. Bannenberg, E. Herdtweck, R. Schmid, *Organometallics* **2005**, *24*, 3163.
[22] J. J. Bahl, R. B. Bates, W. A. Beavers, C. R. Launer, *J. Am. Chem. Soc.* **1977**, *99*, 6126.
[23] P. v. R. Schleyer, D. Wilhelm, T. Clark, *J. Organomet. Chem.* **1985**, *281*, C17.
[24] A. Shortland, G. Wilkinson, *J. Chem. Soc., Chem. Commun.* **1972**, 318.
[25] V. Pfennig, K. Seppelt, *Science* **1996**, *271*, 626.
[26] A. W. Ehlers, G. Frenking, *J. Am. Chem. Soc.* **1994**, *116*, 1514.
[27] B. Delly, M. Wrinn, H. P. Lüthi, *J. Chem. Phys.* **1994**, *100*, 5785.
[28] J. Li, G. Schreckenbach, T. Ziegler, *J. Am. Chem. Soc.* **1995**, *117*, 486.
[29] V. Jonas, W. Thiel, *J. Phys. Chem.* **1995**, *102*, 8474.
[30] T. A. Barckholtz, B. E. Bursten, *J. Am. Chem. Soc.* **1998**, *120*, 1926.
[31] S. Niu, M. B. Hall, *Chem. Rev.* **2000**, *100*, 353.
[32] P. Macchi, A. Sironi, *Coord. Chem. Rev.* **2003**, *238*, 383.
[33] J.-L. Carreon, J. N. Harvey, *Phys. Chem. Chem. Phys.* **2006**, *8*, 93.
[34] A. D. Becke, *J. Chem. Phys.* **1993**, *98*, 5648.
[35] C. Lee, W. Yang, R. G. Parr, *Phys. Rev. B* **1988**, *37*, 785.
[36] A. D. Becke, *Phys. Rev. A* **1988**, *38*, 3098.
[37] J. P. Perdew, *Phys. Rev. B* **1986**, *33*, 8822.
[38] See especially F. Fourche, J. P. Perdew, *J. Chem. Phys.* **2006**, *124*, 044103.
[39] H.-Y. Wang, Y. Xie, R. B. King, H. F. Schaefer, *J. Am. Chem. Soc.* **2006**, *128*, 11376.
[40] M. J. Frisch, G. W. Trucks, H. B. Schlegel, G. E. Scuseria, M. A. Robb, J. R. Cheeseman, J. A. Montgomery, Jr., T. Vreven, K. N. Kudin, J. C. Burant, J. M. Millam, S. S. Iyengar, J. Tomasi, V. Barone, B. Mennucci, M. Cossi, G. Scalmani, N. Rega, G. A. Petersson, H. Nakatsuji, M. Hada, M. Ehara, K. Toyota, R. Fukuda, J. Hasegawa, M. Ishida, T. Nakajima, Y. Honda, O. Kitao, H. Nakai, M. Klene, X. Li, J. E. Knox, H. P. Hratchian, J. B. Cross, C. Adamo, J. Jaramillo, R. Gomperts, R. E. Stratmann, O. Yazyev, A. J. Austin, R. Cammi, C. Pomelli, J. W. Ochterski, P. Y. Ayala, K. Morokuma, G. A. Voth, P. Salvador, J. J. Dannenberg, V. G. Zakrzewski, S. Dapprich, A. D. Daniels, M. C. Strain, O. Farkas, D. K. Malick, A. D. Rabuck, K. Raghavachari, J. B. Foresman, J. V. Ortiz, Q. Cui, A. G. Baboul, S. Clifford, J. Cioslowski, B. B. Stefanov, G. Liu, A. Liashenko, P. Piskorz, I. Komaromi, R. L. Martin, D. J. Fox, T. Keith, M. A. Al-Laham, C. Y. Peng, A. Nanayakkara, M. Challacombe, P. M. W. Gill, B. Johnson, W. Chen, M. W. Wong, C. Gonzalez, J. A. Pople, *Gaussian 03*, Gaussian, Inc., Pittsburgh PA, **2003**..
[41] T. H. Dunning, *J. Chem. Phys.* **1970**, *53*, 2823.
[42] S. Huzinaga, *J. Chem. Phys.* **1965**, *42*, 1293.
[43] A. J. H. Wachters, *J. Chem. Phys.* **1970**, *52*, 1033.
[44] D. M. Hood, R. M. Pitzer, H. F. Schaefer, *J. Chem. Phys.* **1979**, *71*, 705.
[45] B. N. Papas, H. F. Schaefer, *J. Mol. Struct.* **2006**, *768*, 275.
[46] Y. Xie, H. F. Schaefer, R. B. King, *J. Am. Chem. Soc.* **2000**, *122*, 8746.
[47] J. D. Zeinstra, J. L. De Boer, *J. Organomet. Chem.* **1973**, *54*, 207.
[48] L. T. Reynolds, G. Wilkinson, *J. Inorg. Nucl. Chem.* **1958**, *9*, 86.
[49] G. Wilke, B. Bogdanović, *Angew. Chem.* **1961**, *73*, 756.
[50] T. Arliguie, M. Lance, M. Nierlich, J. Vigner, M. Ephritikhine, *J. Chem. Soc., Chem. Commun.* **1995**, 183.

Received: March 23, 2008
Published Online: July 9, 2008

